

Special Issue: THIESEL2024



Effects of bio-derived oxygenated fuel molecules on emission reduction by a three-way catalyst during combustion in a direct-injection spark ignition engine

International J of Engine Research
1–12
© IMechE 2025
© P
Article reuse guidelines:
sagepub.com/journals-permissions
DOI: 10.1177/14680874251353365
journals.sagepub.com/home/jer

Viktor Kärcher, Paul Hellier and Nicos Ladommatos

Abstract

The displacement of fossil fuel use for transport with sustainable alternatives is urgently required to reduce greenhouse gas emissions and address global climate change. Advanced biofuels from renewable feedstocks, for example waste biomass, present an opportunity to decarbonise the use of combustion for propulsion however sustainable utilisation of these fuels also requires consideration of impacts on other exhaust pollutants that negatively affect the environment and human health. Therefore, while exhaust after-treatment systems are an established and effective means of emission reduction during combustion of hydrocarbon fuels, there is a need to understand impacts of biofuel use on the performance of devices including three-way catalysts (TWC) for simultaneous reduction of nitrogen oxides (NOx), carbon monoxide (CO) and unburnt hydrocarbons (THC). This experimental study therefore investigates the effects of four potential biofuel molecules, 2-methylfuran (MF), 2-methyltetrahydrofuran (MTHF), gamma valerolactone (GVL) and linalool (LNL), on combustion, engine-out exhaust emissions and pollutant conversion across a three-way catalyst (TWC) in a gasoline direct-injection engine. The potential biofuel molecules were blended with reference gasoline (RGL) at 20% wt/wt and supplied to a light-duty direct-injection spark ignition engine operated at constant conditions, with gaseous and particulate exhaust emissions measured pre- and post- TWC during catalyst warm-up during engine cold-start and at steady state. While the biofuel blends displayed similar rates of heat release rate relative to gasoline combustion, the MF blend significantly increased CO and NOx engine-out emissions both during cold-start and at steady state. The use of GVL reduced NOx, while hydrogen (H₂) emissions correlated with blend hydrogen carbon ratio. All of the biofuel blends increased the TWC inlet temperature required for pollutant conversion, while MF, LNL and GVL increased H₂ levels post-TWC at higher temperatures. LNL exhibited higher particulate levels post-TWC than gasoline only, despite lower engine-out emissions during combustion of the biofuel blend.

Keywords

After-treatment, biofuels, furan, three-way catalyst, exhaust emissions, particulates, spark ignition

Date received: 7 November 2024; accepted: 11 June 2025

Introduction

The urgent need to address global climate change¹ and achieve net-zero carbon emission requires the displacement of fossil fuels in transport with renewable alternatives.²⁻⁴ Liquid fuels from bio-derived feedstocks and synthetic fuels produced from zero-carbon electricity provide an opportunity to progress the decarbonisation of various transport sectors while utilising existing infrastructure and vehicle fleets.⁵ However, an important challenge in realising the sustainable use of alternative fuels in internal combustion (IC) engines for

transport is the minimisation of pollutant emissions detrimental to air quality and public health.⁶ While exhaust after-treatment devices have been optimised for the reduction of pollutant emissions from the use of

Department of Mechanical Engineering, University College London, London, UK

Corresponding author:

Paul Hellier, Department of Mechanical Engineering, University College London, Roberts Building, Torrington Place, London WCIE 7JE, UK. Email: p.hellier@ucl.ac.uk hydrocarbon-based fossil-derived fuels in compliance with current and upcoming legislative limits, there is a need to understand how the introduction of renewable fuels of varying composition impact the efficiency of these systems.^{7,8}

The conversion of lignocellulosic biomass to liquid compounds with potential use as drop-in fuels for both spark ignition and compression ignition engines has received significant attention; in the context of production processes^{9–13} and also effects on engine combustion and emissions during utilisation. 14-17 Such fuels potentially present lesser impact on land-use and greater net reductions in greenhouse gas emissions than current widely used biofuels, namely ethanol and fatty acid methyl ester biodiesel. ¹⁸ Various processes have been developed for the conversion of lignocellulosic biomass to furfural, a platform chemical suitable for onwards transformation to various high-value chemicals and potential renewable fuels. 19 The use of furfural as a drop-in fuel is limited by unfavourable physical properties and sequential steps of hydrogenation can be applied to reduce fuel bound oxygen resulting in species including 2-methylfuran (MF) and 2-methyltetrahydrofuran (MTHF).²⁰ Other processing routes can result in species incorporating alternative oxygenated functional groups, for example acyclic alcohols and lactones. 20,21

Three-way catalysts (TWC) have been widely utilised for spark ignition engines operating with stoichiometric air fuel mixtures since the introduction of exhaust emissions limits to achieve the simultaneous reduction of nitrogen oxides (NOx) alongside oxidation of carbon monoxide (CO) and total unburnt hydrocarbons (THC).²² While these were initially developed for non-oxygen bearing gasoline fuels consisting of various hydrocarbon species, several previous studies have investigated the effect of fuel composition on TWC performance, primarily ethanol gasoline blends and for which varying effects of fuel oxygen have been observed.^{23–26}

Iodice et al.²⁷ investigated the reduction of pollutants by a TWC with ethanol gasoline blends of varying composition. At hot catalyst conditions increasing fuel ethanol content consistently increased pollutant reduction by TWC, attributed to lower engine out levels via more complete combustion, however, less consistent effects were observed during cold-start, with a 30% ethanol in gasoline blend increasing CO and HC levels post- TWC. Kärcher et al.²⁸ investigating the effects of hydrogen (H₂) addition upstream of a TWC, and also synergies with fuel composition, found that use of ethanol and butanol gasoline blends resulted in reduced conversion temperatures for up to 1500 ppm H₂, while larger and cyclic oxygenates showed an opposing effect. Sinha Majumdar et al.²⁹ and Ladshaw et al.³⁰ investigated and modelled the impact of various oxygenates on an aged TWC in a synthetic exhaust flow reactor. Experiments were undertaken with fixed fuel concentrations of 3000 ppmC in the synthetic exhaust gas and oxygen flowrates varied so as to achieve constant lambda values (λ). The presence of short-chain acyclic oxygenates in the synthetic exhaust gas decreased the light-off temperature of the TWC for conversion of CO, THC and NOx, while increases in TWC light-off temperature were observed with the presence of aromatics and cyclic oxygenates.

This paper presents the results of novel engine experiments investigating the effects of four potential bio-derived fuel molecules on TWC emission conversion when present during combustion in a directinjection spark ignition engine. The potential biofuel molecules included two furans, a lactone ester and long-chain alcohol, representative of a range of potential fuels from lignocellulosic biomass. While the combustion characteristics of these biofuel molecules have been investigated previously,^{31–35} this study is the first to systematically investigate effects of these fuels on TWC performance in an engine test bed. The molecules were tested during engine warm-up and steady state conditions as 20% (wt/wt) blends with a fossil gasoline, with measurements of in-cylinder pressure, engine-out emissions and TWC reduction of regulated pollutants, CO, THC, NOx, particle number (PN) and particle mass (PM) and H_2 .

Experimental methodology

Engine and catalyst test facility

All experiments were undertaken with a modified VW 1.4L TSI engine, operated with three firing and one motored cylinder. The engine had been modified for research use with separate intake and exhaust manifolds for the three firing cylinders and single motored cylinder. Fuel was supplied to the three firing cylinders from a 4.3 L fuel tank compressed by nitrogen via the original manufacturer high-pressure fuel pump and common rail. Fuel was injected to each cylinder via 6hole solenoid injectors (Magneti Marelli) and control of injection parameters determined through the PC interface of the engine control unit (ECU). In-cylinder gas pressure was measured at a resolution of 0.4 crank angle degrees (CAD) by a water-cooled, piezoelectric pressure transducer (Kistler 6061BS31) and recorded by a bespoke data acquisition system (National Instruments Labview). Engine exhaust gas from the three firing cylinders was passed through a TWC with emissions measurement upstream and downstream of the catalyst. A schematic overview of the engine and catalyst test facility is shown in Figure 1, while Table 1 lists the engine specification.

A commercially available Euro VI compliant ceramic brick TWC was utilised and had been previously de-greened until steady state performance reached, with Table 2 showing the TWC parameters. Exhaust gas temperature and λ were measured at the inlet to the TWC, with measurement and sampling ports placed within 150 to 200 mm either upstream or downstream

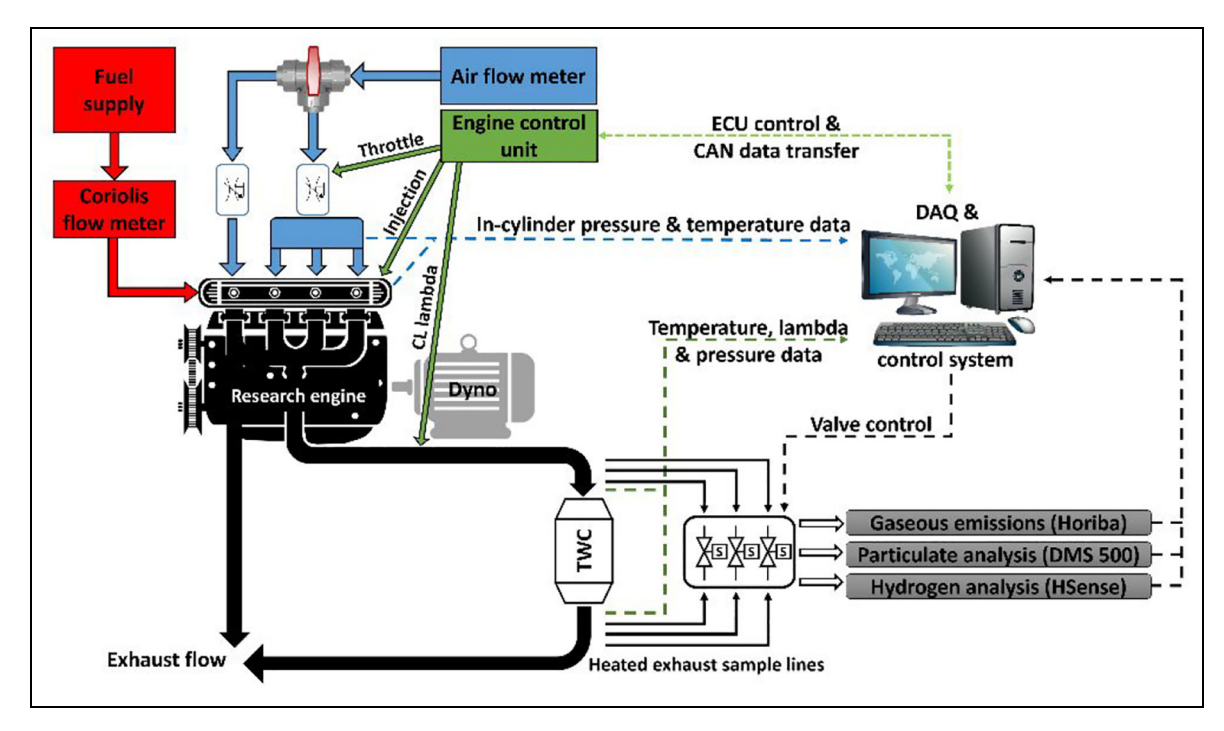


Figure 1. Schematic representation of the engine and catalyst test facility.

Table 1. Engine specification.

Number of cylinders	4
Bore (mm)	76.5
Stroke (mm)	75.6
Swept volume/cylinder (cm ³)	347.5
Compression ratio	10:1
DI fuel injectors	6-hole solenoid
Coolant temperature (°C)	82 \pm 4
Oil temperature (°C)	80 ± 2

of the TWC. Concurrent measurements of gaseous emissions (CO, CO₂, THC and NOx) were made both upstream (pre-) and downstream (post-) of the TWC by Horiba Mexa 9100 and 9400 automotive emissions analysers via separate PID controlled heated lines at a constant temperature of 190°C. Measurements of H₂ concentration and particulate emissions were undertaken via further heated lines in immediately consecutive experiments (due to analyser availability) by V&F Hsense electron impact mass spectrometer and Cambustion DMS500 fast particulate spectrometer respectively.

Fuels investigated

Four potential biofuel molecules, 2-methylfuran (MF), 2-methyltetrahydrofuran (MTHF), gamma valerolactone (GVL) and linalool (LNL), were tested as 20% gravimetric (wt/wt) blends with a reference gasoline (RGL). The molecules were selected as representative of molecules feasibly achieved from lignocellulosic

Table 2. Properties of the ceramic TWC brick.

Catalyst type	3-way – Pd/Rh/Pt
Base material	Cordierite
PGM ratio	19/5/1
PGM loading (g)	15
Ø of element (mm)	101
Length of element (mm)	76
Volume (L)	0.61
Cell density (cpsi)	400
Wall thickness (mm)	0.15

biomass and also to provide insight into the following effects of fuel molecular structure:

- 1. Degree of saturation in a furan ring, MTHF relative to MF.
- Addition of a ketone group, GVL relative to MTHF.

All of the single component molecules were obtained from a chemical supplier (Sigma Aldrich) at an assay of 96% or greater, while the reference gasoline (Carcal RF-02-03) was fossil derived and obtained from a fuels supplier (Haltermann-Carless). A constant 20% blending proportion of each single component molecule with reference gasoline was selected to maximise potential fuel effects on engine emissions and TWC performance, while maintaining compatibility of the blends with the fuel injection system. The molecular structure of the potential biofuel molecules is shown in Table 3, while Table 4 lists the properties of all fuels tested.

Table 3. Fuel molecular structures.

Experimental conditions

Each of the fuel blends and reference gasoline were tested at constant engine operating conditions of 1600 rpm, 4.7 bar indicated mean effective pressure (IMEP) and exhaust lambda value (λ) of between 0.995 and 0.997. The throttle position was adjusted for each fuel so as to achieve a constant IMEP for all tests of 4.77 ± 0.02 bar, while the engine was operated in a closed-loop lambda mode, with a 1 Hz 2.5% lambda perturbation. For all tests, fuels were injected at a timing of 280 CAD before top-dead centre (BTDC) and pressure of 80 bar with the injection duration determined by the closed loop control. A spark timing of 15 CAD BTDC was used for all tests, while every experiment included a 12 second period of operation on start-up at 900 rpm for stabilisation and heating of the closed-loop lambda probe. Measurements were taken both during an initial cold-start phase of 300 s following engine start-up for each test and also subsequently at steady-state conditions. A summary of the experimental and engine operating conditions specific to each fuel is shown in Table 5.

Results and discussion

Combustion characteristics

Figure 2 shows the in-cylinder pressure, apparent net heat release rate and mass fraction burnt (MFB) of the 20% potential biofuel molecule blends with gasoline and also the reference gasoline. Readily apparent from Figure 2 is that addition of 20% of the potential biofuel molecules did not significantly impact combustion phasing, however, it can be seen that, with the exception of the 20% GVL blend, all of the fuel blends resulted in an elevated in-cylinder pressure (Figure 2(a)). This is in agreement with the slightly higher engine IMEP during the fuel blend tests (Table 5), however, it is interesting to note that the GVL blend produced the highest relative IMEP (4.79 vs 4.75 bar) and widest opening throttle position. Figure 2(b) shows an earlier increasing heat release rate for the potential biofuel blends relative to reference gasoline following ignition, with the exception of the GVL blend and in agreement with the observed lower in-cylinder pressure (Figure 2(a)) and later time of occurrence of 5, 10, 50 and 90% mass fraction burnt (Figure 2(c). Of the fuel blends, the fastest increase in heat release rate is apparent in the case of MF (Figure 2(b)), in agreement with previous studies of MF as a single component fuel where faster combustion relative to RGL was observed. 31,32 In shock tube experiments by Jouzdani et al.,33 MTHF was found to display longer ignition delay times than MF, attributed to the presence of weaker C-H bonds more susceptible to radical attack in the unsaturated furan and in agreement with the slower rates of heat release rate increase apparent in Figure 2(b). The higher heat release rates of MTHF relative to GVL are in contrast to the study of Talibi et al.34 where in blends with ethanol and gasoline the furan displayed lower rates of heat release. This work, however, utilised a carburetter for fuel delivery within the engine intake manifold, suggesting a greater influence of the elevated boiling point and density of the lactone relative to the furan in the current study employing high-pressure direct injection of the fuels. Also utilising a carburetter for fuel delivery, Hellier et al.³⁵ observed an initial increase in peak heat release rate with the addition of 10% linalool to gasoline, similar to the increase apparent in Figure 2(b), but a level

Table 4. Fuel properties.

Fuel	Molecular formula	AFR _{st} ^a	H/C	Oxygen (%)	T _{boil} (°C) ³⁶	Density (kg/dm ³) ³⁶	Assay (%)
Reference gasoline	-	14.22	1.73	0.92	-	0.747	-
2-methylfuran	C_5H_6O	10.11	1.2	19.49	65	0.913	98
2-methyltetrahydrofuran	$C_5H_{10}O$	11.24	2.0	18.57	78	0.855	99
Linalool	C ₁₀ H ₁₈ O	12.55	1.6	10.37	198 ³⁵	0.867	96
Gamma-valerolactone	$C_5H_8O_2$	8.29	1.8	31.96	219	1.079	99

^aCalculated according to the method of Spicher et al.³⁷

Engine operating conditions for oxygenated fuel blends and gasoline.

Fuel	Injection du	njection duration (ms)	Throttle pos	sition (%)	Intake manifo	ntake manifold pressure (bar)	Lambda (λ)	Fuel flow (g/min)	g/min)	IMEP (bar)	(-
	Mean	lσ	Mean	lσ	Mean	Ισ		Mean	lσ	Mean	lσ
Reference gasoline 2-methylfuran 2-methyltetrahydrofuran Linalool Gamma-valarolartone	1.667 1.738 1.718 1.733	0.006 0.0012 0.015 0.011	7.62 7.63 7.56 7.59	0.03 0.05 0.05 0.05	0.641 0.639 0.633 0.633	0.028 0.028 0.028 0.028	0.995 0.996 0.995 0.997	29.05 30.67 30.29 30.76	0.14 0.22 0.23 0.23	4.75 8.74 7.74 7.74	0.03 0.04 0.04 0.04
Garrilla-Yarer Olaccorie	100:1	200	01.1	10.0	2000	0.020	00	25:35	2.0	1.1.7	

of peak heat release lower than gasoline with a blend of 40% LNL.

Engine-out emissions

Figure 3 shows the engine-out gaseous emissions from the 20% fuel blends and reference gasoline during the engine cold-start period, and at steady-state relative to the boiling point of the potential biofuel molecule present in each blend. Where shown in Figure 3 and subsequent figures, the data points indicate mean values and the error bars one standard deviation from the mean. In Figure 3(a), it can be seen both furan blends, those of MF and MTHF, exhibited appreciably higher levels of CO during engine cold-start relative to the LNL and GVL blends, and reference gasoline. Most pronounced are the higher levels of CO emitted by MF, displaying both a lesser initial decrease following engine start-up and a greater increase during 100 to 250s of engine operation. Levels of engine-out H₂ (Figure 3(b)) were however similar for all fuels tested, with the greatest deviation displayed by the LNL blend between 50 and 100 s during cold-start.

Figure 3(c) shows the engine-out measurements of THC, with significantly higher levels emitted by LNL and GVL throughout engine cold-start, while both furan blends produced lower THC than the reference gasoline, as observed in previous tests of MF and MTHF gasoline blends. 38,39 Readily apparent from Figure 3(c) is the correlation between fuel blend component boiling point and THC, with the two molecules of highest boiling point, GVL and LNL, emitting significantly higher levels throughout relative to the lower boiling point furans (Table 4). The higher boiling points of GVL and LNL may have reduced rates of vaporisation and efficiency of fuel air mixing during the compression stroke, resulting in a less homogenous mixture and greater persistence of unburnt fuel.⁴⁰ In Figure 3(d), it can be seen that for all fuels levels of NOx emitted increased during engine cold-start, with the highest levels throughout displayed by the MF blend and the lowest by GVL. This is in agreement with previous studies of MF³⁸ and the observed lower peak in-cylinder pressure and slower increase in heat release rate of the GVL blend (Figure 2), with both characteristics likely to reduce the magnitude of in-cylinder temperatures where the majority of NOx is expected to form through thermal oxidation of nitrogen, the rates of which are highly sensitive to temperature. 40,41

Figure 4 shows the engine-out particulate emissions from the 20% fuel blends and reference gasoline during the engine cold-start period, and at steady-state relative to the boiling point of the potential biofuel molecule present in each blend. Immediately apparent from Figure 4(a) is the significant reduction in particle number (PN) for all of the potential biofuel molecule blends throughout the engine cold-start period relative to RGL, with the largest reductions apparent from GVL

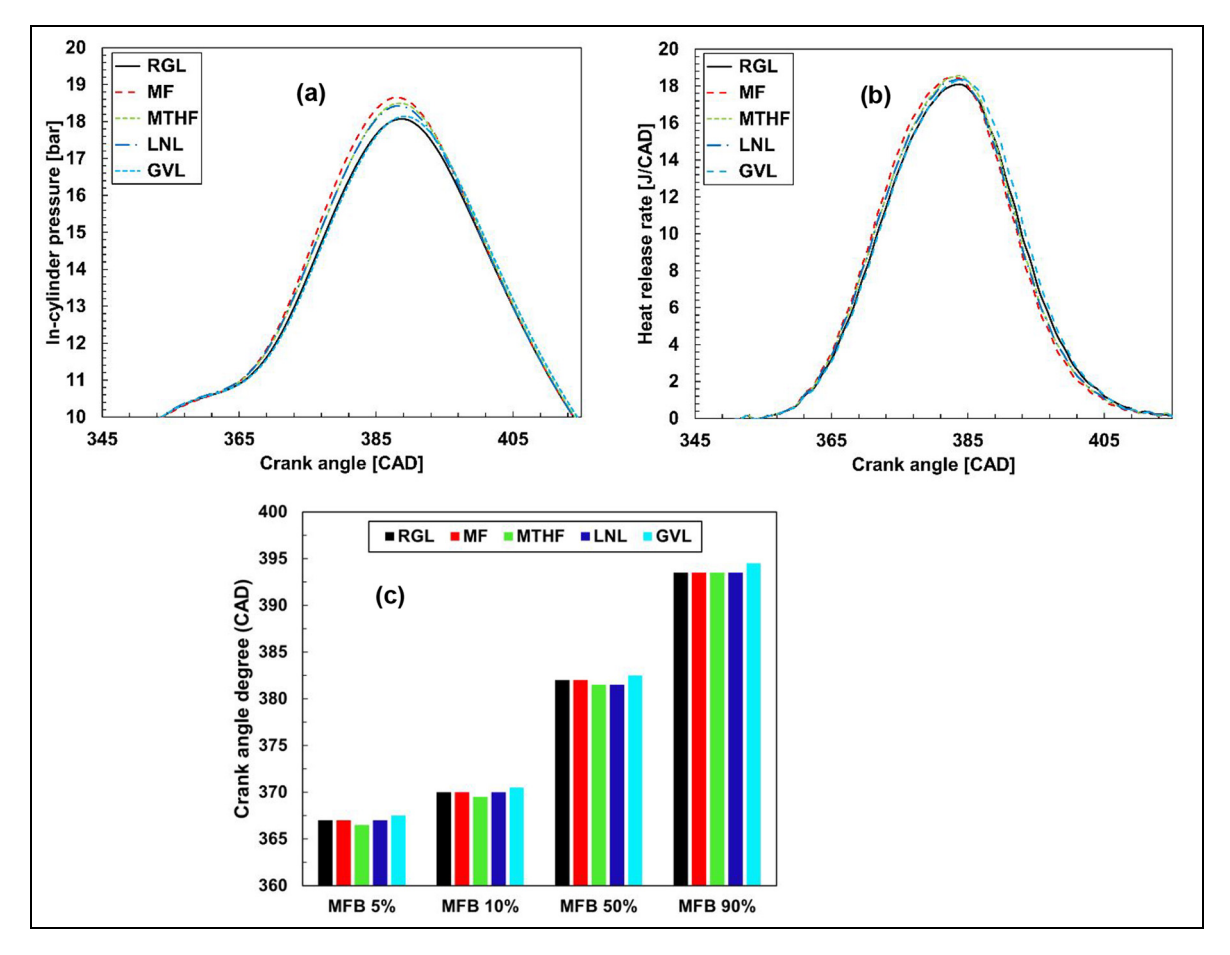


Figure 2. (a) In-cylinder pressure, (b) apparent net heat release rate and (c) time of occurrence of mass fraction burnt of 20% (wt/wt) fuel blends and reference gasoline at steady-state operation following engine cold-start.

and MTHF. It is suggested that the especially high oxygen content of GVL inhibited particle formation through limiting the availability of carbon atoms for production of soot precursors, 42 while the greater reduction of PN displayed by MTHF relative to MF can potentially be attributed to the aromatic character of the later. 43 In Figure 4(b), it can be seen that all of the potential biofuel blends exhibited lower particle mass (PM) levels during cold-start relative to RGL, with the exception of LNL. While the blends of MTHF, GVL and MF all displayed a rapid decrease in the level of PM emitted during the first 100s of coldstart, levels of PM emitted by LNL did not show significant decrease until after 100s (later than exhibited by RGL), only reducing to a level below that of RGL between 225 and 250 s after engine start.

Figure 5 shows the particle number size distribution measured in the engine-out exhaust during combustion of the 20% fuel blends and reference gasoline at steady-state, following cold-start. It can be seen that all of the potential biofuel molecule blends exhibited a lower peak particle number than RGL, found

at a similar particle diameter of 10 to 20 nm for all fuels tested (Figure 5).

TWC emissions conversion

Figure 6 shows the exhaust H₂ concentration post-TWC during combustion of the potential biofuel molecule blends and RGL during engine cold-start. It can be seen that while H₂ levels initially remain similar for all fuels, with near complete conversion by 120 s, subsequently levels from LNL, GVL and MF increase appreciably, deviating from RGL and MTHF. The most significant increase is exhibited by LNL, increasing to approximately 800 ppm H₂ at 180 s, while H₂ levels post- TWC from MF decrease to a similar level as exhibited by RGL at 300s (Figure 6). This is in contrast to the engine-out, pre- TWC H₂ levels measured (Figure 3(b)), which remained similar for all fuels during the cold-start period. It is suggested that the higher densities of LNL, GVL and MF relative to RGL (Table 4) may have reduced access to the active sites within the TWC washcoat, reducing conversion

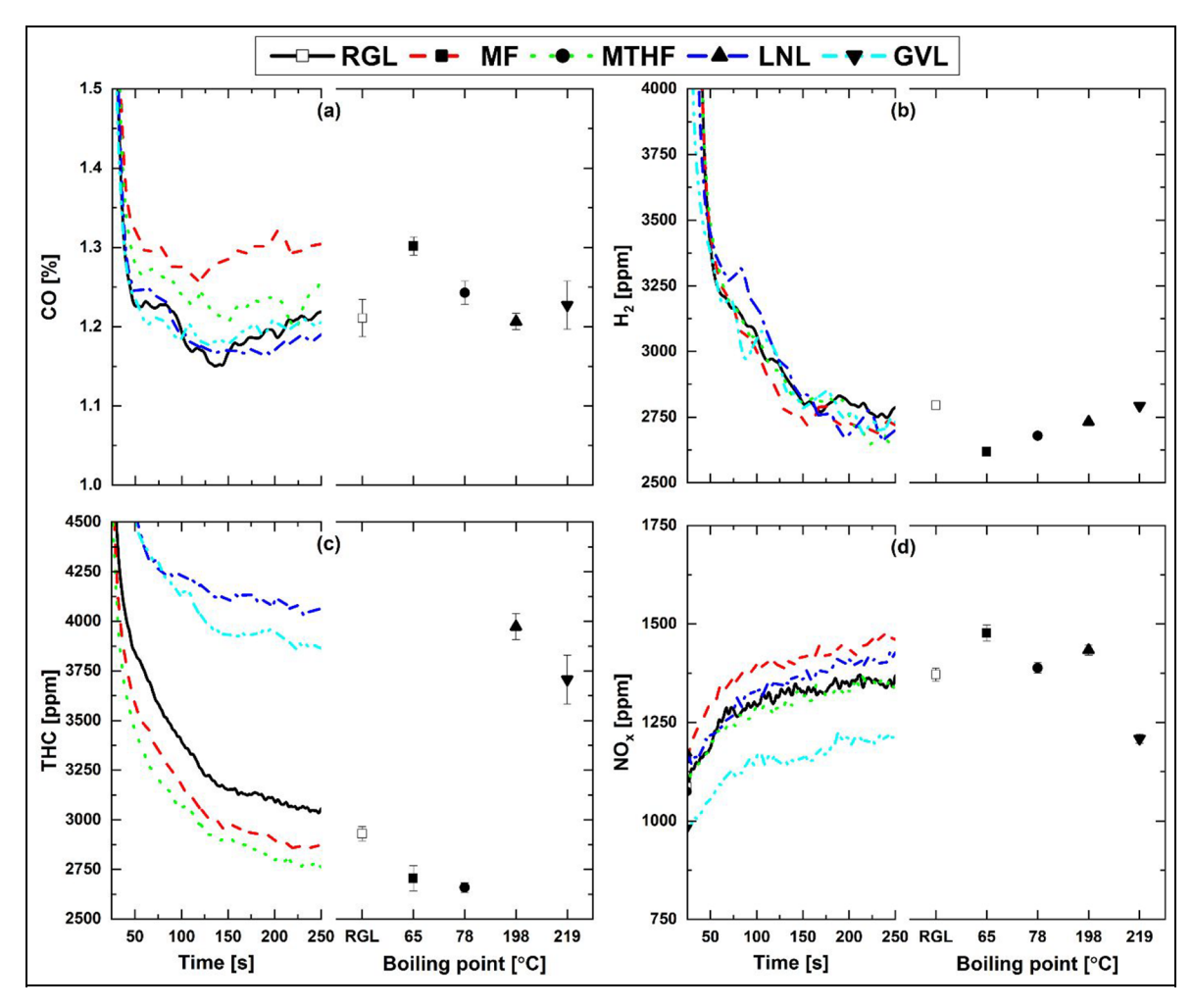


Figure 3. (a) CO, (b) H_2 , (c) THC and (d) NOx engine out emissions from 20% (wt/wt) fuel blends and reference gasoline during cold-start and at steady-state operation relative to blend component boiling point.

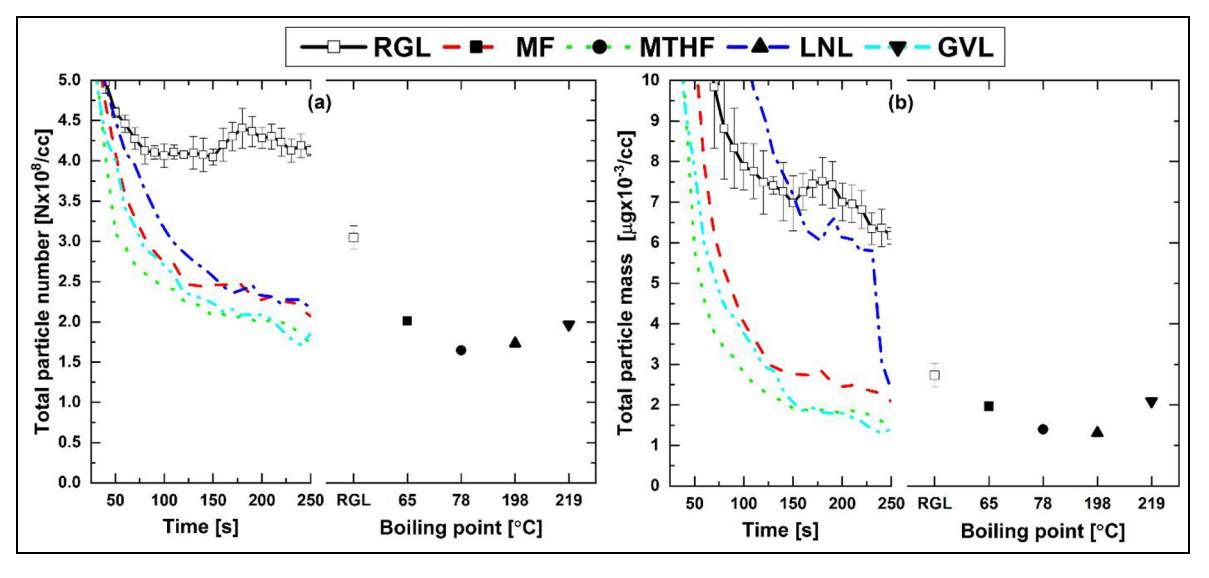


Figure 4. (a) Total particle number and (b) total particle mass engine-out emissions from 20% (wt/wt) fuel blends and reference gasoline during cold-start and at steady-state operation relative to blend component boiling point.

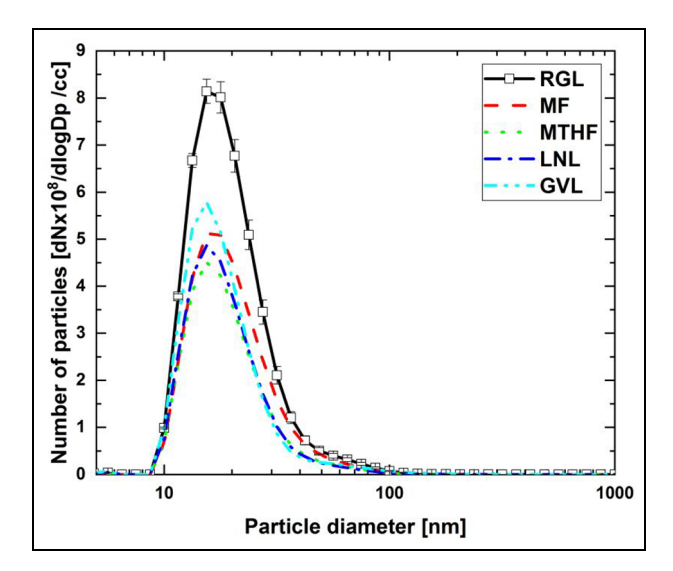


Figure 5. Engine-out particle number size distribution from 20% (wt/wt) fuel blends and reference gasoline steady-state operation.

capability. The higher density and molecular weight, of these molecules may have decreased diffusion rates of these species, impeding access and conversion of H₂, especially during lower temperature operation of the TWC earlier in the cold-start period. An additional possibility in the case of LNL and GVL is that higher engine out THC (Figure 3(c)) may have increased H₂ formation across the TWC (Figure 6) via the water-gas shift reaction. Furthermore, the higher levels of H₂ across the TWC during operation with LNL and GVL (Figure 6) may have exacerbated the formation of NH₃ and N₂O, 45,46 especially so LNL which also emitted among the highest levels of engine out NOx (Figure 3(d)).

Figure 7 shows the change in TWC inlet exhaust gas temperature required for the conversion of 0.6% CO, 600 ppm NOx and 1200 ppm THC during combustion of the potential biofuel molecule blends relative to the same level of absolute pollutant species conversion during operation with RGL. It can be seen from Figure 7 that use of all of the potential biofuel molecule blends required an increase in the TWC inlet temperature of between 1°C and 9.5°C for pollutant reduction relative to RGL, suggesting reduced conversion efficiency in all cases. LNL and GVL required the largest increases in TWC inlet temperature of ~9.5°C and ~7.5°C for conversion of CO, while the same level of reduction was achieved through increases of 2.5°C and 1.5°C for the unsaturated and saturated furans respectively. For conversion of 600 ppm of NOx, the largest temperature increase of ~6.5°C was required for MTHF, with an increase of only 2°C necessary for the same conversion with MF (Figure 7). Overall, the increase in TWC inlet temperature required for conversion of 1200 ppm THC relative to RGL was less for all fuel blends relative to

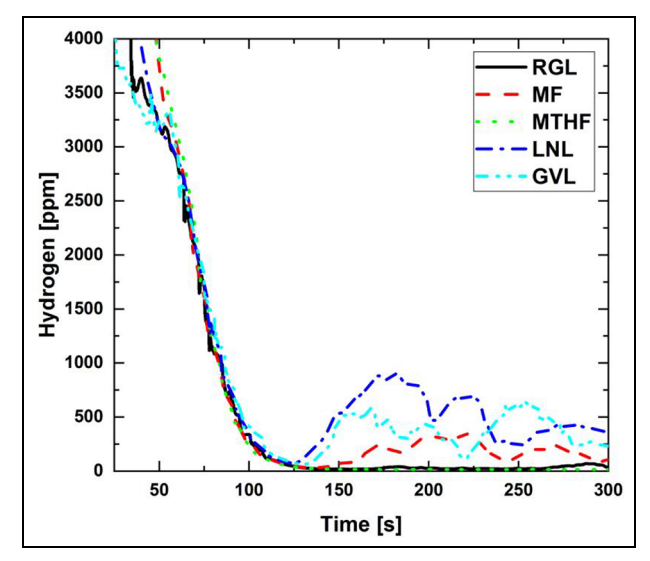


Figure 6. H₂ concentrations post- TWC from 20% (wt/wt) fuel blends and reference gasoline during engine cold-start.

that necessary for CO and NOx, with both furans displaying an increase of \sim 2.5°C and LNL and GVL showing \sim 3.5°C increase.

In comparing Figures 3 and 7, it can be seen that GVL required an increase in the TWC inlet temperature for conversion of 600 ppm NOx despite producing lower engine-out NOx than RGL (Figure 3(d)), suggesting a direct effect of fuel composition; as opposed to effects arising from combustion related changes in engine-out exhaust gas composition. A similar observation, albeit to a lesser extent, can be made when considering the lower THC engine-out emissions of both furans relative to RGL (Figure 3(c)) with an increase of ~2°C required in TWC inlet temperature for conversion of 1200 ppm THC (Figure 7).

Figure 8 shows the total PN and PM emissions post-TWC from the potential biofuel molecule fuel blends and RGL during cold-start and at steady-state relative to the fuel component density. In Figure 8(a), it can be seen that PN levels post- TWC decreased throughout the cold-start period for all fuels except LNL and, to a lesser extent, GVL. Also apparent is that from approximately 100s onwards (Figure 8(a)), PN levels post-TWC are significantly reduced compared to engineout, pre-TWC, where the PN concentration for all fuels remained above 1.5×10^8 per cc (Figure 4(a)). Figure 8(b) shows a similar effect of fuel composition, with higher post-TWC PM from LNL and GVL relative to RGL and both furan blends. With the exception of LNL, a reduction in PM across the TWC is also apparent (Figures 4(b) and 8(b)), albeit to a much lesser extent than observed in PN, highlighting the greater efficacy of the TWC in the oxidation of smaller nucleation mode particles which impact less on total particle mass.47,48 No clear effect of fuel component density is

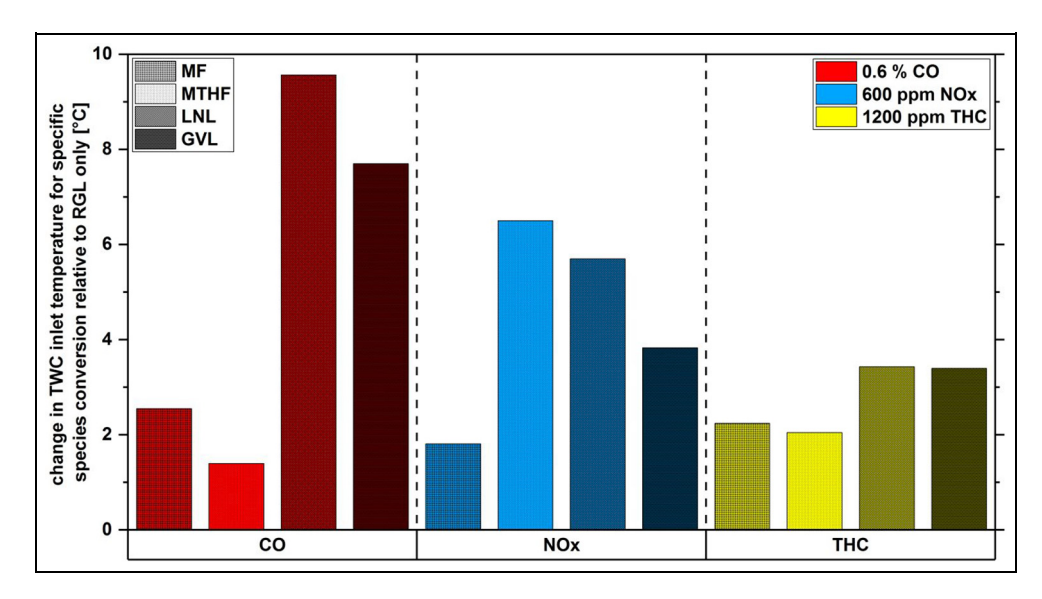


Figure 7. Change in TWC inlet temperature required for consuming 0.6%, 600 ppm and 1200 ppm of CO, NOx and THC respectively for 20% (wt/wt) fuel blends, identified by graded shading in the legend, relative to RGL.

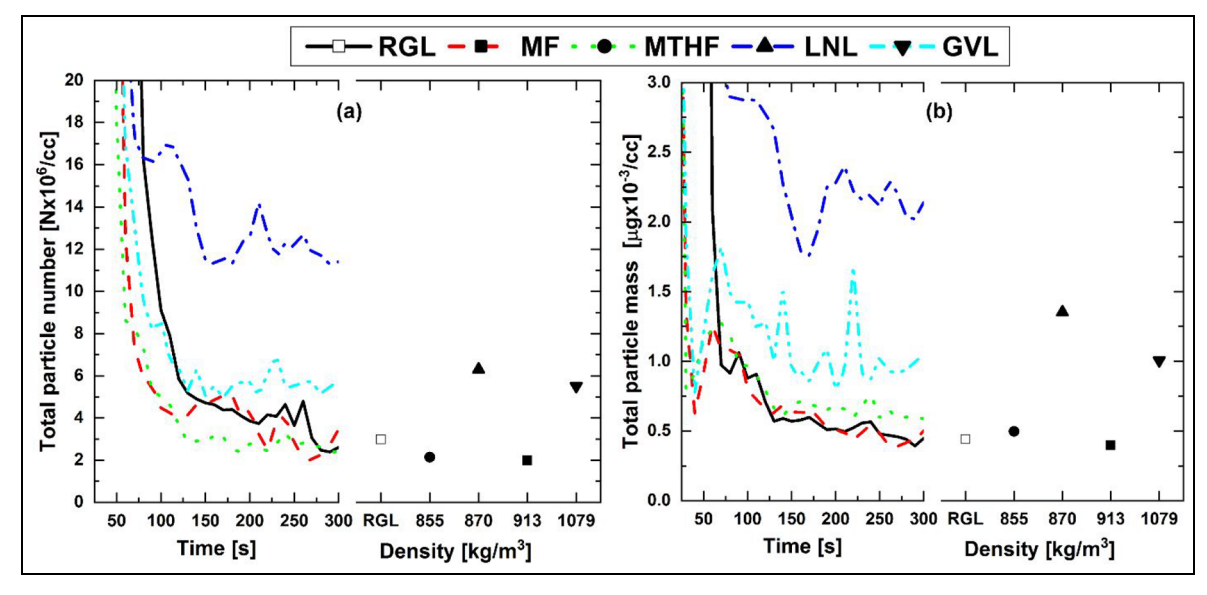


Figure 8. (a) Total particle number and (b) total particle mass post-TWC from 20% (wt/wt) fuel blends and reference gasoline during cold-start and at steady-state operation relative to blend component density.

apparent in Figure 8, potentially suggesting no significant contribution of liquid fuel droplets in the PN concentrations recorded.

Figure 9 shows the particle number size distribution and median nucleation and accumulation mode particle diameters post-TWC from the potential biofuel molecule fuel blends and RGL at steady-state relative. Apparent from Figure 9(a) are the larger peak particle numbers from LNL and GVL relative to RGL in both nucleation and accumulation mode size ranges. Both furans, MF and MTHF, however, exhibited lower peak

particle numbers, with no clear effect of the furan ring saturation (Figure 9(a)). It can also be seen that relative to engine-out, pre-TWC (Figure 5), peak particle numbers in the nucleation mode size range are significantly reduced for all blends (Figure 9(a)) in agreement with expected soot oxidation by the TWC, ⁴⁹ though this effect is diminished by the presence of 20% LNL and GVL. Figure 9(b). shows a decrease in accumulation mode median particle diameter with increasing fuel blend component density, with that of the GVL blend similar to RGL only.

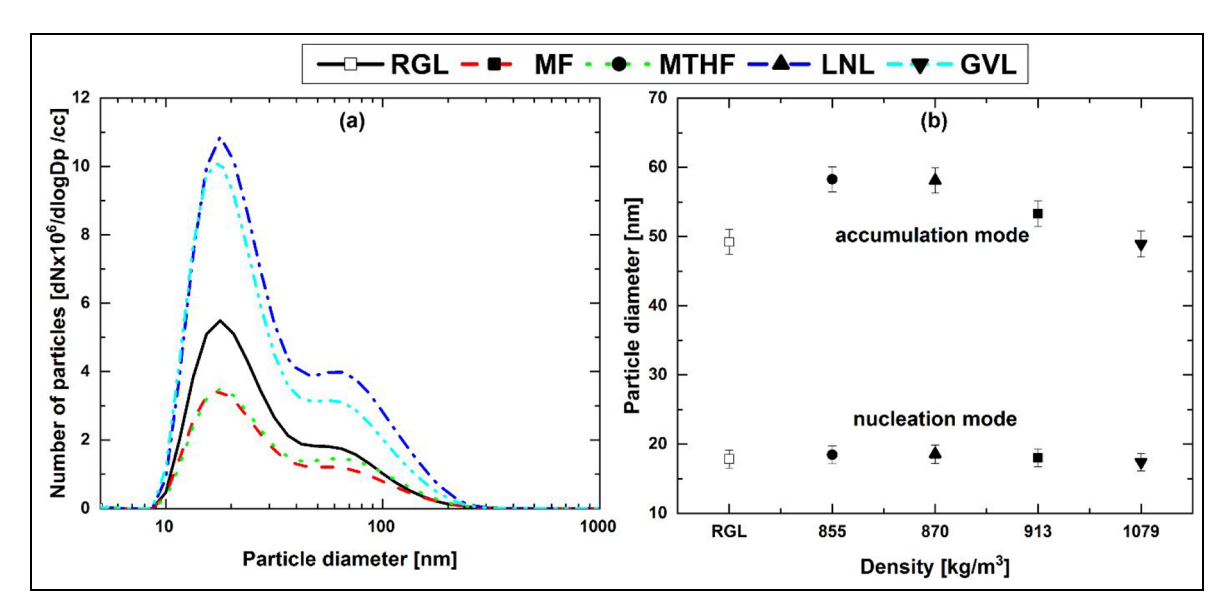


Figure 9. (a) Particle number size distribution and (b) median nucleation mode and accumulation mode particle diameters against fuel component density post-TWC from 20% (wt/wt) fuel blends and reference gasoline at steady-state operation.

Conclusions

Four potential oxygenated biofuel molecules, MF, MTHF, GVL and LNL, were tested in a direct-injection spark ignition engine as 20% blends with reference gasoline. From observation of fuel effects during both engine cold-start and steady-state operation, the following specific conclusions in relation to combustion characteristics, engine-out emissions and TWC conversion performance can be drawn:

- All four potential biofuel molecules resulted in an increase in TWC inlet temperature required for the conversion of absolute amounts of CO, THC and NOx relative to RGL, even when displaying lower engine-out emissions. Post- TWC levels of H₂ increased for LNL, GVL and MF following an initial decrease during engine cold-start, attributed to the higher density and molecular weight of the oxygenate molecules.
- 2. During engine cold-start, PN levels were reduced downstream of the TWC for all fuels, albeit to a lesser extent for LNL, the molecule of lowest oxygen content of those investigated. The peak number of nucleation mode particles was reduced by the TWC for all fuels relative to that of accumulation mode particles, with a fuel effect apparent in GVL and LNL displaying higher peak particle numbers than RGL despite lower engine-out levels.
- 3. Addition of 20% MF, MTHF and LNL increased peak heat release rates during combustion relative to RGL. However, the GVL blend reduced

- combustion speed and delayed peak heat release relative to RGL, with the denser lactone blend requiring a higher fuel flowrate and wider throttle opening position for an equivalent engine IMEP.
- 4. Both furan blends increased engine-out CO but decreased THC levels relative to RGL, while the use of LNL and GVL appreciably increased THC. Emissions of NOx were primarily influenced by changes in combustion phasing and thermal conditions produced by varying fuel composition, while all of the oxygenated fuels reduced engine-out PN during cold-start.

The results of this study demonstrate the importance of investigating synergies between renewable fuel composition and the performance of exhaust aftertreatment systems, especially during engine cold-start where the introduction of all the oxygenated molecules tested increased TWC inlet temperatures for equivalent pollutant reduction. In addition, the diverse range of oxygenate molecular structures investigated highlights the potential feasibility of these as drop-in fuels where after-treatment systems have been developed accordingly, for example to avoid inadvertent increases in PN. Future work is required to gain fundamental understanding of the changes in reaction routes and rates within catalytic after-treatment systems with the use of oxygenated biofuels. Meanwhile, further work towards the practical uptake of such renewable fuels in conjunction with after-treatment systems should consider effects of varying blend levels and long-term catalyst performance.

Declaration of conflicting interests

The author(s) declared no potential conflicts of interest with respect to the research, authorship, and/or publication of this article.

Funding

The author(s) disclosed receipt of the following financial support for the research, authorship, and/or publication of this article: The authors wish to acknowledge the financial support of the UK Engineering and Physical Sciences Reseach Council, EPSRC Grant EP/M007960/1.

ORCID iD

Paul Hellier (b) https://orcid.org/0000-0001-9836-0511

References

- 1. Falk J, Colwell RR, Behera SK, et al. An urgent need for COP27: confronting converging crises. *Sustain Sci* 2023; 18: 1059–1063.
- Cheng F, Luo H, Jenkins JD and Larson ED. The value of low- and negative-carbon fuels in the transition to netzero emission economies: lifecycle greenhouse gas emissions and cost assessments across multiple fuel types. *Appl Energy* 2023; 331: 120388.
- Khan MZA, Khan HA, Ravi SS, Turner JW and Aziz M. Potential of clean liquid fuels in decarbonizing transportation – an overlooked net- zero pathway? *Renew* Sustain Energ Rev 2023; 183: 113483.
- 4. Curran S, Onorati A, Payri R, et al. The future of ship engines: Renewable fuels and enabling technologies for decarbonization. *Int J Engine Res* 2024; 25: 85–110.
- Duarte Souza Alvarenga Santos N, Rückert Roso V, Teixeira Malaquias AC and Coelho Baêta JG. Internal combustion engines and biofuels: examining why this robust combination should not be ignored for future sustainable transportation. *Renew Sustain Energ Rev* 2021; 148: 111292.
- 6. Yim SH and Barrett SR. Public health impacts of combustion emissions in the United Kingdom. *Environ Sci Technol* 2012; 46: 4291–4296.
- Morgan C and Goodwin J. Impact of the proposed Euro
 Regulations on exhaust aftertreatment system design.
 Johnson Matthey Technol Rev 2023; 67: 239–245.
- Yanowitz J, Christensen E and Mccormick RL. Utilization of renewable oxygenates as gasoline blending components. National Renewable Energy Laboratory, http://www.nrel.gov/docs/fy11osti/50791.pdf (2011, accessed 31 July 2017).
- 9. Alonso DM, Wettstein SG and Dumesic JA. Bimetallic catalysts for upgrading of biomass to fuels and chemicals. *Chem Soc Rev* 2012; 41: 8075–8098.
- Zhou C-H, Xia X, Lin C-X, Tong DS and Beltramini J. Catalytic conversion of lignocellulosic biomass to fine chemicals and fuels. *Chem Soc Rev* 2011; 40: 5588–5617.
- Rodionova MV, Bozieva AM, Zharmukhamedov SK, et al. A comprehensive review on lignocellulosic biomass biorefinery for sustainable biofuel production. *Int J Hydrogen Energy* 2022; 47: 1481–1498.
- 12. Okolie JA, Mukherjee A, Nanda S, Dalai AK and Kozinski JA. Next-generation biofuels and platform

- biochemicals from lignocellulosic biomass. *Int J Energy Res* 2021; 45: 14145–14169.
- 13. Ashokkumar V, Venkatkarthick R, Jayashree S, et al. Recent advances in lignocellulosic biomass for biofuels and value-added bioproducts a critical review. *Bioresour Technol* 2022; 344: 126195.
- Sudholt A, Cai L, Heyne J, et al. Ignition characteristics of a bio-derived class of saturated and unsaturated furans for engine applications. *Proc Combust Inst* 2015; 35: 2957–2965
- 15. Frost J, Hellier P and Ladommatos N. A systematic study into the effect of lignocellulose-derived biofuels on the combustion and emissions of fossil diesel blends in a compression ignition engine. *Fuel* 2022; 313: 122663.
- 16. Tian M, McCormick RL, Ratcliff MA, et al. Performance of lignin derived compounds as octane boosters. *Fuel* 2017; 189: 284–292.
- 17. Koivisto E, Ladommatos N and Gold M. Compression ignition and exhaust gas emissions of fuel molecules which can Be produced from lignocellulosic biomass: levulinates, valeric esters, and ketones. *Energy Fuels* 2015; 29: 5875–5884.
- Bilal M, Wang Z, Cui J, et al. Environmental impact of lignocellulosic wastes and their effective exploitation as smart carriers – a drive towards greener and eco-friendlier biocatalytic systems. Sci Total Environ 2020; 722: 137903.
- Adhami W, Richel A and Len C. A review of recent advances in the production of furfural in batch system. *Mol Catal* 2023; 545: 113178.
- 20. Lange JP, van der Heide E, van Buijtenen J and Price R. Furfural-a promising platform for lignocellulosic biofuels. *ChemSusChem* 2012; 5: 150–166.
- 21. Alonso DM, Wettstein SG and Dumesic JA. Gamma-valerolactone, a sustainable platform molecule derived from lignocellulosic biomass. *Green Chem* 2013; 15: 584.
- Granger P and Parvulescu VI. Catalytic NOx abatement systems for mobile sources: from three-way to lean burn after-treatment technologies. *Chem Rev* 2011; 111: 3155–3207.
- 23. Jin D, Choi K, Myung CL, et al. The impact of various ethanol-gasoline blends on particulates and unregulated gaseous emissions characteristics from a spark ignition direct injection (SIDI) passenger vehicle. *Fuel* 2017; 209: 702–712.
- Suarez-Bertoa R, Zardini AA, Keuken H and Astorga C. Impact of ethanol containing gasoline blends on emissions from a flex-fuel vehicle tested over the worldwide harmonized Light duty Test Cycle (WLTC). *Fuel* 2015; 143: 173–182.
- Schifter I, González U, Díaz L, et al. From actual ethanol contents in gasoline to mid-blends and E-85 in conventional technology vehicles. Emission control issues and consequences. *Fuel* 2018; 219: 239–247.
- 26. Falcão Weissinger F, Henrique Rufino C, Mendoza AP, et al. Electrically heated catalyst enabling pollutants reduction in hybrid vehicles fueled with ethanol. *Int J Engine Res* 2024; 25: 850–863.
- 27. Iodice P, Langella G and Amoresano A. Ethanol in gasoline fuel blends: effect on fuel consumption and engine out emissions of SI engines in cold operating conditions. *Appl Therm Eng* 2018; 130: 1081–1089.
- 28. Kärcher V, Hellier P and Ladommatos N. Effects of exhaust gas hydrogen addition and oxygenated fuel blends on the light-off performance of a three-way

- catalyst. SAE Powertrains, Fuels and Lubricants, 2019, 2019-01-2329.
- Sinha Majumdar S, Pihl JA and Toops TJ. Reactivity of novel high-performance fuels on commercial three-way catalysts for control of emissions from spark-ignition engines. *Appl Energy* 2019; 255: 113640.
- Ladshaw AP, Majumdar SS and Pihl JA. Experiments and modeling to evaluate global reaction kinetics of three-way catalyst light off for net-zero carbon fuels and selected fuel blends. *Appl Catal B Environ* 2023; 324: 122281.
- 31. Thewes M, Muether M, Pischinger S, et al. Analysis of the impact of 2-methylfuran on mixture formation and combustion in a direct-injection spark-ignition engine. *Energy Fuels* 2011; 25: 5549–5561.
- 32. Liu H, Olalere R, Wang C, Ma X and Xu H. Combustion characteristics and engine performance of 2-methylfuran compared to gasoline and ethanol in a direct injection spark ignition engine. *Fuel* 2021; 299: 120825.
- Jouzdani S, Eldeeb MA, Zhang L and Akih-Kumgeh B. High-temperature study of 2-methyl furan and 2-methyl tetrahydrofuran combustion. *Int J Chem Kinet* 2016; 48: 491–503.
- 34. Talibi M, Hellier P and Ladommatos N. Investigating the combustion and emissions characteristics of biomass-derived platform fuels as gasoline extenders in a single cylinder spark-ignition engine. SAE technical paper 2017-01–2325, 2017.
- Hellier P, Al-Haj L, Talibi M, Purton S and Ladommatos N. Combustion and emissions characterization of terpenes with a view to their biological production in cyanobacteria. *Fuel* 2013; 111: 670–688.
- Awad OI, Mamat R, Ibrahim TK, et al. Overview of the oxygenated fuels in spark ignition engine: environmental and performance. *Renew Sustain Energ Rev* 2018; 91: 394–408.
- Spicher U, Bernhardt S, Meinig U, et al. Ladungswechsel. In: van Basshuysen R and Schäfer F (eds) Handbuch Verbrennungsmotor: Grundlagen, Komponenten, Systeme, Perspektiven. Wiesbaden: Springer Fachmedien Wiesbaden, 2015, pp.465–532.
- 38. Wang C, Xu H, Daniel R, et al. Combustion characteristics and emissions of 2-methylfuran compared to 2,5-dimethylfuran, gasoline and ethanol in a DISI engine. *Fuel* 2013; 103: 200–211.
- Olalere RK, Zhang G and Xu H. Experimental investigation of gaseous emissions and hydrocarbon speciation for MF and MTHF gasoline blends in DISI engine. *Int J Automot Manuf Mater* 2024; 3: 6.
- Heywood JB (ed.). Internal Combustion Engine Fundamentals. 2nd ed. New York: McGraw-Hill Education, 2014.
- 41. Zeldovich YB, Sadavnikov PY and Frank-Kamentskii DA. *Oxidation of nitrogen in combustion*. Moscow: Acad Sci USSR, 1947.
- 42. Eveleigh A, Ladommatos N, Hellier P and Jourdan AL. Quantification of the fraction of particulate matter derived from a range of ¹³C-labeled fuels blended into heptane, studied in a diesel engine and Tube Reactor. *Energy Fuels* 2016; 30: 7678–7690.
- 43. Kholghy MR, Weingarten J, Sediako AD, et al. Structural effects of biodiesel on soot formation in a laminar

- coflow diffusion flame. *Proc Combust Inst* 2017; 36: 1321–1328.
- 44. Whittington B, Jiang CJ and Trimm DL. Vehicle exhaust catalysis: I. The relative importance of catalytic oxidation, steam reforming and water-gas shift reactions. *Catal Today* 1995; 26: 41–45.
- De Abreu Goes J, Woo JW and Olsson L. Effects of feed gas composition on fresh and aged TWC-coated GPFs loaded with real soot. *Ind Eng Chem Res* 2020; 59: 10790– 10803.
- 46. Bae WB, Kim DY, Byun SW, et al. Emission of NH3 and N2O during NO reduction over commercial aged three-way catalyst (TWC): role of individual reductants in simulated exhausts. *Chem Eng J Adv* 2022; 9: 100222.
- 47. Bogarra M, Herreros JM, Hergueta C, et al. Influence of three-way catalyst on gaseous and particulate matter emissions during gasoline direct injection engine cold-start. *Johnson Matthey Technol Rev* 2017; 61: 329–341.
- 48. Whelan I, Timoney D, Smith W and Samuel S. The effect of a three-way catalytic converter on particulate matter from a gasoline direct-injection engine during cold-start. *SAE Int J Engines* 2013; 6: 1035–1045.
- 49. Suteerapongpun T, Ogura M and Hanamura K. A multilayer membrane filter made of potassium catalyst and three-way catalyst for a passive after-treatment system. *Int J Engine Res* 2024; 25: 1991–2000.

Appendix

Notation

TWCThree-way catalyst. NOxNitrogen oxides. CO_2 Carbon dioxide. COCarbon monoxide. THCTotal unburnt hydrocarbons. H_2 Hydrogen. MF2-methylfuran. MTHF2-methyltetrahydrofuran. GVLGamma valerolactone.

LNL Linalool.

RGL Reference gasoline.

IMEP Indicated mean effective pressure.

λ Exhaust lambda value.
 PN Particle number.
 PM Particle mass.
 CAD Crank angle degree.
 BTDC Before top dead centre.
 PGM Platinum group metals.
 MFB Mass fraction burnt.

Ø Diameter.

cpsi Cells per square inch. *AFR_{st}* Stoichiometric air fuel ratio.

 T_{boil} Boiling temperature. σ Standard deviation.